

AN EXPERIMENTAL PLATFORM FOR VALIDATING INTERNAL ACTUATOR CONTROL STRATEGIES

Chris Schultz^{*,1} Craig Woolsey^{*,1}

** Department of Aerospace & Ocean Engineering
Virginia Polytechnic Institute and State University
Blacksburg, VA 24061-0203 USA
{cschultz,cwoolsey}@vt.edu*

Abstract: Internal actuators, such as moving mass actuators and reaction wheels, have been proposed as attitude control devices for autonomous underwater vehicles. This paper describes modeling and design of a modular, internally actuated autonomous underwater vehicle. The vehicle design allows for a variety of internal actuator modules and external fairings. The base body is a spherical glass pressure housing which contains an internal actuator module, sensors, and an on-board computer. The first actuator module, comprising three reaction wheel actuators, will provide a unique facility for investigating nonlinear spacecraft attitude control as well as underwater vehicle control. *Copyright ©2003 IFAC*

Keywords: Autonomous vehicles, nonlinear systems, rotors, space vehicles

1. INTRODUCTION

Low-speed attitude control is required for basic autonomous underwater vehicle (AUV) tasks such as docking and inspection. Internal actuators are appealing for this application because they may expand an AUV's performance envelope while improving reliability and efficiency. Conventional streamlined AUV's include a thruster for propulsion and fins for attitude control. Fins lose control effectiveness at low speed, however, so controllability in hover requires additional actuators. External thrusters are effective for low speed control, but

they add drag when the vehicle moves at higher speeds. Because internal actuators do not rely on relative fluid motion to exert control moments, they can be used to control a vehicle's attitude at low speeds. Moreover, internal actuators are protected from corrosion, fouling, and other damage and they require no hull penetrations for power or control signals.

An alternative idea which has been proposed for low-speed attitude control of AUV's is articulated "pectoral" fins (Kato and Tadahiko, 1998). A related idea, dubbed the "oscillating fin thruster," has already been implemented on the streamlined underwater vehicle Morpheus (Hobson *et al.*, 2002). While this type of actuator is quite promising, it suf-

¹ This work was sponsored in part by the National Science Foundation under Grant CMS-0133210 and by the Office of Naval Research under Grant N00014-01-1-0588.

fers the same susceptibility to corrosion, biological fouling, and other damage as do more conventional external actuators. It is therefore of interest to consider the utility of internal actuators.

In fact, a number of AUV's already use internal actuators. Underwater gliders typically use a servo-actuated internal mass to shift their center of gravity. (See (Leonard and Graver, 2001) and references contained there.) Internal rotors have also been used to provide gyroscopic stability for ships and as "momentum wheels" for attitude control of remotely operated underwater cameras. To the authors' knowledge, "reaction wheel" actuators, which use momentum exchange to control vehicle attitude, have not been implemented for underwater vehicle control. Analysis suggests, however, that reaction wheels could be effective actuators, particularly for streamlined vehicles moving at low speeds (Woolsey and Leonard, 2002).

The development of control algorithms for AUV's with internal actuators is of both practical and theoretical interest. From a control theoretical perspective, internally actuated vehicles are of interest because they are underactuated; that is, they have fewer actuators than degrees of freedom. Such vehicles typically are not linearly controllable and therefore they require a more sophisticated, nonlinear approach to control design. The problem of controlling underactuated AUV's has motivated fundamental theory on nonlinear control synthesis and stabilization.



Fig. 1. IAMBUS

This paper describes modeling, design, and construction of the Internally Actuated, Modular Bodied, Untethered Submersible (IAMBUS). The purpose of this laboratory-scale AUV is the experimental validation of vehicle control strategies using internal actuators. The vehicle can accommodate various internal actuator modules, including internal rotors, a moving mass, or a control moment gyroscope. The first actuator module is a trio of orthogonal reaction wheels. The vehicle base body is a spherical glass pressure housing, which contains the internal actuator module, an on-board computer,

and sensors. The base body's hydrodynamic characteristics can be modified by mounting it within an external fairing.

While the ultimate purpose of the experimental platform is to investigate AUV control, the spherical base body provides a unique platform for studying spacecraft attitude control. Because the instrument housing is spherical, there is no hydrodynamic coupling and very little rotational drag. Moreover, the vehicle can perform arbitrary slewing maneuvers, whereas typical spacecraft attitude simulators have a restricted range of motion (Schwartz *et al.*, 2003). Initial experiments will demonstrate IAMBUS' utility for investigating nonlinear attitude control schemes.

In Section 2, we discuss dynamic modeling for an AUV with internal rotor actuators. In Section 3, we describe the vehicle design, emphasizing important trade-offs which arise when using internal rotors. We conclude in Section 4.

2. DYNAMIC MODELING

In this section, we describe modeling for an AUV with internal rotor actuators. In Section 2.1, we describe the general case. In Section 2.2, we specialize to the case of a spherical body which rotates without translating. In this latter case, we describe how IAMBUS can be used to investigate nonlinear spacecraft attitude control.

2.1 Dynamics of an AUV with Internal Rotors

Figure 2 depicts a rigid hull, immersed in a perfect fluid, which contains three axisymmetric internal rotors. An orthonormal coordinate frame $(\mathbf{b}_1, \mathbf{b}_2, \mathbf{b}_3)$ is fixed to a point in the hull. It is assumed that the rotors are mounted orthogonally within the hull such that their symmetry axes intersect at the body coordinate origin. Without further loss of generality, the body coordinate axes can be chosen collinear with the rotor spin axes. Another orthonormal coordinate frame $(\mathbf{i}_1, \mathbf{i}_2, \mathbf{i}_3)$ is fixed in space. These two coordinate frames are related by a proper rotation matrix \mathbf{R} , which describes the attitude of the hull with respect to the inertial coordinate frame, and an inertial vector \mathbf{x} , which denotes the position of the body coordinate origin with respect to the inertial coordinate origin. Any point \mathbf{x}_B expressed with respect to body coordinates

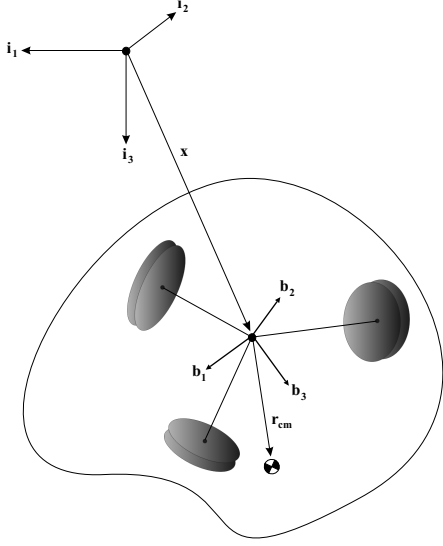


Fig. 2. Rigid body with internal rotors.

can be transformed to inertial coordinates according to the relation

$$\mathbf{x}_I = \mathbf{R}\mathbf{x}_B + \mathbf{x}.$$

Let $\boldsymbol{\phi} = [\phi_1, \phi_2, \phi_3]^T$ denote the vector of rotor spin angles, measured relative to the body-fixed coordinate frame. The three-tuple $(\mathbf{R}, \mathbf{x}, \boldsymbol{\phi})$ completely describes the system configuration.

Kinematic equations. Suppose that the rigid hull rotates with instantaneous angular velocity $\boldsymbol{\Omega}$, expressed in body coordinates, and translates with velocity \mathbf{v} , also expressed in body coordinates. Let $\boldsymbol{\Omega}_r = \frac{d}{dt}\boldsymbol{\phi}$. The kinematic equations relate the system configuration $(\mathbf{R}, \mathbf{x}, \boldsymbol{\phi})$ to the system velocity $(\boldsymbol{\Omega}, \mathbf{v}, \boldsymbol{\Omega}_r)$. To express this relationship, we first define the operator $\hat{\cdot}$ such that

$$\hat{\mathbf{y}} = \begin{pmatrix} 0 & -y_3 & y_2 \\ y_3 & 0 & -y_1 \\ -y_2 & y_1 & 0 \end{pmatrix}$$

for $\mathbf{y} \in \mathbb{R}^3$. Notice that $\hat{\mathbf{y}}\mathbf{z} = \mathbf{y} \times \mathbf{z}$ for vectors $\mathbf{y}, \mathbf{z} \in \mathbb{R}^3$. With the definition above, we may write the complete kinematic equations as

$$\begin{aligned} \dot{\mathbf{R}} &= \mathbf{R}\hat{\boldsymbol{\Omega}} \\ \dot{\mathbf{x}} &= \mathbf{R}\mathbf{v} \\ \dot{\boldsymbol{\phi}} &= \boldsymbol{\Omega}_r. \end{aligned} \quad (1)$$

Dynamic equations. Denote by $\boldsymbol{\Pi}$ the total angular momentum of the system about the body coordinate origin, expressed in body coordinates. Similarly, let \mathbf{P} represent the total translational

momentum in body coordinates. Finally, let \mathbf{L} be the vector whose components are the total angular momenta of the three internal rotors about their spin axes, also expressed in body coordinates. These momenta may be computed from the system's kinetic energy, which includes contributions due the hull and rotor motion and to the induced motion of the fluid.

The rigid body contribution to the total kinetic energy depends on the vehicle mass distribution. Let m represent the vehicle mass and let the body coordinate vector \mathbf{r}_{cm} denote the location of the vehicle center of mass. Let $\boldsymbol{\Lambda}_{\text{RB}}$ represent the rigid body *locked inertia matrix*. This is the inertia matrix, computed in the body coordinate frame, in the case that all of the rotors are locked in place. Finally, let J_i represent the moment of inertia of the i^{th} internal rotor about its spin axis and define $\mathbf{J} = \text{diag}(J_1, J_2, J_3)$. These parameters are sufficient to define the rigid body component of kinetic energy.

The fluid contribution to the total kinetic energy is defined by a quadratic form whose elements are the added inertia matrix \mathbf{I}_F , the added mass matrix \mathbf{M}_F , and the hydrodynamic coupling matrix \mathbf{C}_F . The elements of these matrices are computed as described in (Lamb, 1932).

The total system kinetic energy is $K =$

$$\frac{1}{2} \begin{pmatrix} \boldsymbol{\Omega} \\ \mathbf{v} \\ \boldsymbol{\Omega}_r \end{pmatrix} \cdot \begin{pmatrix} \boldsymbol{\Lambda} & \mathbf{C} & \mathbf{J} \\ \mathbf{C}^T & \mathbf{M} & \mathbf{0} \\ \mathbf{J} & \mathbf{0} & \mathbf{J} \end{pmatrix} \begin{pmatrix} \boldsymbol{\Omega} \\ \mathbf{v} \\ \boldsymbol{\Omega}_r \end{pmatrix},$$

where

$$\begin{aligned} \boldsymbol{\Lambda} &= \boldsymbol{\Lambda}_{\text{RB}} + \mathbf{I}_F \\ \mathbf{C} &= m\hat{\mathbf{r}}_{\text{cm}} + \mathbf{C}_F \\ \mathbf{M} &= m\mathbb{I} + \mathbf{M}_F \end{aligned}$$

and where \mathbb{I} represents the 3×3 identity matrix. The momenta $\boldsymbol{\Pi}$, \mathbf{P} , and \mathbf{L} are computed from the total kinetic energy as follows

$$\begin{aligned} \boldsymbol{\Pi} &= \frac{\partial K}{\partial \boldsymbol{\Omega}} = \boldsymbol{\Lambda}\boldsymbol{\Omega} + \mathbf{C}\mathbf{v} + \mathbf{J}\boldsymbol{\Omega}_r \\ \mathbf{P} &= \frac{\partial K}{\partial \mathbf{v}} = \mathbf{C}^T\boldsymbol{\Omega} + \mathbf{M}\mathbf{v} \\ \mathbf{L} &= \frac{\partial K}{\partial \boldsymbol{\Omega}_r} = \mathbf{J}\boldsymbol{\Omega} + \mathbf{J}\boldsymbol{\Omega}_r. \end{aligned}$$

The dynamic equations relate the rate of change of these momenta to the external forces and torques acting on the system.

The vehicle is assumed to be neutrally buoyant. Let $\mathbf{F}_{\text{ext}_1} = mg\mathbf{i}_3$ represent the weight of the vehicle and $\mathbf{F}_{\text{ext}_2} = -mg\mathbf{i}_3$ represent the equal and opposite buoyant force. Let $\mathbf{F}_{\text{ext}_i}$ represent an external point force which acts at the point \mathbf{r}_i , where both vectors are expressed in body coordinates and where $i \in \{3, \dots, I\}$. Similarly, let $\mathbf{T}_{\text{ext}_j}$ represent a pure external torque acting on the system, expressed in body coordinates, where $j \in \{1, \dots, J\}$. Finally, let $\mathbf{T}_{\text{int}_k}$ represent a vector whose components are internal torques acting about the spin axes of the three rotors, where $k \in \{1, \dots, K\}$. The complete equations of motion, with the effects of gravity and buoyancy represented explicitly, are

$$\begin{aligned}
\dot{\mathbf{R}} &= \mathbf{R}\hat{\boldsymbol{\Omega}} \\
\dot{\mathbf{b}} &= \mathbf{R}\mathbf{v} \\
\dot{\boldsymbol{\phi}} &= \boldsymbol{\Omega}_r \\
\dot{\boldsymbol{\Pi}} &= \boldsymbol{\Pi} \times \boldsymbol{\Omega} + \mathbf{P} \times \mathbf{v} + \mathbf{r}_{\text{cm}} \times (mg\mathbf{R}^T\mathbf{i}_3) \\
&\quad + \sum_{i=3}^I \mathbf{r}_i \times \mathbf{F}_{\text{ext}_i} + \sum_{j=1}^J \mathbf{T}_{\text{ext}_j} \\
\dot{\mathbf{P}} &= \mathbf{P} \times \boldsymbol{\Omega} + \sum_{i=3}^I \mathbf{F}_{\text{ext}_i} \\
\dot{\mathbf{L}} &= \mathbf{L} \times \boldsymbol{\Omega} + \sum_{k=1}^K \mathbf{T}_{\text{int}_k}. \tag{2}
\end{aligned}$$

2.2 Special Case: Spacecraft Attitude Simulator

Under special conditions, the underwater vehicle model described in Section 2.1 reduces to the standard model for a rotating rigid body. Assume that the neutrally buoyant vehicle has a spherical hull and that it is trimmed such that the center of gravity lies at the center of buoyancy. In this case, the gravitational torque acting on the vehicle vanishes. Moreover, because the vehicle hull is spherical, there is neither added inertia ($\mathbf{I}_F = \mathbf{0}$) nor hydrodynamic coupling ($\mathbf{C}_F = \mathbf{0}$) and the rotational damping is negligibly small for small angular rates. Assume further that gravity and buoyancy are the only external forces or torques acting on the system and that the internal torques on the rotors take the form

$$\sum_{k=1}^K \mathbf{T}_{\text{int}_k} = -\mathbf{D}_{\Omega_r} \boldsymbol{\Omega}_r + \mathbf{u},$$

where $\mathbf{D}_{\Omega_r} = \text{diag}(d_1, d_2, d_3) > 0$ is a matrix of linear damping coefficients and \mathbf{u} is a vector of

control torques. Ignoring the cyclic coordinates $\boldsymbol{\phi}$, the relevant equations of motion become

$$\begin{aligned}
\dot{\mathbf{R}} &= \mathbf{R}\hat{\boldsymbol{\Omega}} \\
\dot{\boldsymbol{\Pi}} &= \boldsymbol{\Pi} \times \boldsymbol{\Omega} \\
\dot{\mathbf{L}} &= \mathbf{L} \times \boldsymbol{\Omega} - \mathbf{D}_{\Omega_r} \boldsymbol{\Omega}_r + \mathbf{u}.
\end{aligned}$$

In the absence of external forces and torques, the magnitude of body angular momentum $\|\boldsymbol{\Pi}(t)\|$ is conserved. Thus, if $\|\boldsymbol{\Pi}(0)\| = 0$, then $\boldsymbol{\Pi}$ is identically zero for all time. In this case, the rotor angular velocity may be expressed directly in terms of the body angular velocity. Solving

$$\mathbf{0} = \boldsymbol{\Pi} = \boldsymbol{\Lambda} \boldsymbol{\Omega} + \mathbf{J} \boldsymbol{\Omega}_r$$

for $\boldsymbol{\Omega}_r$ gives $\boldsymbol{\Omega}_r = -\mathbf{J}^{-1} \boldsymbol{\Lambda} \boldsymbol{\Omega}$. Substituting into the rotor momentum rate equation gives

$$\begin{aligned}
\frac{d}{dt} ((\boldsymbol{\Lambda} - \mathbf{J}) \boldsymbol{\Omega}) &= ((\boldsymbol{\Lambda} - \mathbf{J}) \boldsymbol{\Omega}) \times \boldsymbol{\Omega} \\
&\quad + \mathbf{D}_{\Omega_r} \mathbf{J}^{-1} \boldsymbol{\Lambda} \boldsymbol{\Omega} - \mathbf{u}.
\end{aligned}$$

Let $\mathbf{u} = \mathbf{D}_{\Omega_r} \mathbf{J}^{-1} \boldsymbol{\Lambda} \boldsymbol{\Omega} - \tilde{\mathbf{u}}$ and define a new momentum $\tilde{\boldsymbol{\Pi}} = (\boldsymbol{\Lambda} - \mathbf{J}) \boldsymbol{\Omega}$. The equations of interest become

$$\begin{aligned}
\dot{\mathbf{R}} &= \mathbf{R}\hat{\boldsymbol{\Omega}} \\
\dot{\tilde{\boldsymbol{\Pi}}} &= \tilde{\boldsymbol{\Pi}} \times \boldsymbol{\Omega} + \tilde{\mathbf{u}}
\end{aligned}$$

These are precisely the equations of motion for an externally actuated rigid body modeling, for example, a spacecraft with torque thrusters.

It is anticipated that the spherical base module of IAMBUS will provide a valuable tool for investigating nonlinear spacecraft attitude control strategies. By fixing the spherical module within a spheroidal fairing, one may also investigate the use of reaction wheels to control the attitude of a streamlined underwater vehicle, as described in (Woolsey and Leonard, 2002).

3. DESIGN & CONSTRUCTION

IAMBUS is a modular experimental platform for investigating nonlinear control of vehicles with internal actuators. The platform can support a variety of internal actuator assemblies and external hull shapes. The hull of the base module is a spherical glass pressure housing which is 0.432 meters in diameter. This housing contains the internal actuator

assembly, an active buoyancy control device, a dynamic measurement unit, a PC/104 computer and a DC power supply. The first actuator module consists of three orthogonally mounted reaction wheels; it is shown, partially assembled, in Figure 3.



Fig. 3. The first internal actuator module.

Internal components are secured to a rigid center plate which rests within the lower half of the spherical housing. The center plate fastens to a stand-off ring which rests against the upper half of the housing, supporting the assembly when the vehicle rotates through large angles; see Figure 4. Adjustable trim weights are attached to the four threaded supports connecting the center plate to the stand-off ring. These allow the center of mass to be trimmed such that it coincides with the center of buoyancy.

The vehicle was designed using a computer-aided design (CAD) software package. This allowed the designer to resize and reposition “virtual” components before they were purchased or fabricated. Using CAD software throughout the design process ensured that the final design could be assembled without violating volume, weight, or mass distribution constraints.



Fig. 4. CAD Drawing of IAMBUS.

Actuators. For IAMBUS to be useful as a nonlinear control platform, the internal rotor actuators

must provide sufficient control authority. The criteria for sizing the actuators for attitude control experiments derived from the following performance specification: the spherical base module should execute a complete revolution about a given rotor spin axis, starting and ending at rest, in under 10 seconds. This is a standard approach in spacecraft design for specifying reaction wheel performance (Eterno *et al.*, 1995). Assuming a uniform mass distribution and a minimum time (bang-bang) control law, the necessary torque was computed to be 0.26 Nm. Additional torque is required to offset the viscous damping in the rotor bearing. The motor which was selected is Animatics’ SmartMotor Model 2330. This motor can provide 0.35 Nm of continuous torque and has a maximum speed rating above 5500 rpm. The motor includes an integrated controller/amplifier and optical encoder, which simplifies the vehicle design. The reaction wheel motors communicate serially and can be daisy-chained so that only one serial port is required to control all of the motors.

The two primary factors influencing the internal rotor size were the desire to minimize rotor angular velocity and the requirement that the vehicle be trimmed to neutral buoyancy. Minimizing rotor angular velocity minimizes damping, thereby maximizing the amount of reaction torque which can be delivered to the hull; this observation suggests a rotor with large inertia. The neutral buoyancy requirement imposes a weight limit. Each rotor consists of a cast lead annulus of outer diameter 0.222 meters and inner diameter 0.165 meters, coupled to the motor shaft through a thin aluminum support plate. The outer diameter is the maximum possible, given the geometric limits of the spherical housing. The inner diameter was dictated by the requirement that each rotor have mass less than 2.50 kilograms.

Remark. The sizing of the rotor actuators will impact our later investigation of streamlined AUV stabilization. The destabilizing torque which tends to turn a streamlined vehicle broadside into a relative flow (and thus the control torque necessary to counter it) grows quadratically with velocity. To see this, consider the simple case of translation of a prolate spheroid in a perfect fluid. Assume that the spheroid’s center of gravity coincides with its center of buoyancy. While no drag force acts on the translating spheroid, a moment $\mathbf{P} \times \mathbf{v}$ acts about its center. This torque tends to destabilize steady streamlined translation.

In the limit of a slender spheroid, the maximum value of $\|\mathbf{P} \times \mathbf{v}\|$ is $\frac{1}{4}mV^2$ where V is the nominal

speed. Thus, given the vehicle mass m and a maximum deliverable torque, one may estimate an upper bound on the range of speeds for which streamlined translation can be stabilized using internal actuators. This “speed limit” varies with the square root of the deliverable torque. Thus, internal actuators are most appropriate for low-speed applications. At higher speeds, however, servo-actuated fins are quite capable of generating the control torques necessary to stabilize and steer a streamlined vehicle. In intermediate speed ranges, where both fins and rotors are less effective, control allocation schemes might be devised to provide the necessary control authority. □

The three rotors were balanced using a standard method. The technique involved spinning each rotor at a constant rate and measuring the displacement (magnitude and phase) caused by rotor unbalance. A trial weight was then added to the rotor. The displacement was measured once again and compared with the previous measurement in order to compute the location and increment for a permanent counterweight which would balance the rotor.

The ballast control system comprises a pair of piston-cylinder tanks which are slaved to a single motor, an Animatics SmartMotor Model 2315. The volume of the tanks is sufficient to vary the spherical housing’s submerged weight by $\pm 1\%$. This range is sufficient to trim the vehicle’s depth to a constant value.

Sensors. The sensor suite includes a multi-axis dynamic measurement unit (Systron Donner’s MotionPak II). This sensor provides three axis angular rate in the range $\pm 75^\circ/\text{sec}$ and three axis acceleration in the range $\pm 3g$. The sensor outputs can be read serially or as analog signals. For attitude control experiments, the acceleration and angular rate measurements can be used to obtain the pitch and roll angle. Because experiments are performed in a small steel test tank, reliable heading measurements can not be obtained using a magnetic compass. Currently, heading is estimated by integrating the yaw rate equation. While the estimated signal drifts, as one would expect, the drift rate is slow enough that it does not seriously degrade performance for relatively quick attitude control experiments. A collaborator is currently developing a high frequency long baseline acoustic positioning system which promises to provide accurate position and heading information.

In addition to the dynamic measurement unit, the base vehicle module includes a pressure sensor (Sen-

Sym ICT Model 10C030PA4K). The pressure measurement is used to regulate the vehicle’s depth within the test tank.

On-board computer. The on-board computer is Advanced Micro Peripherals’ Tiny886ULP low power PC/104+ computer. The computer features a 667 MHz Crusoe (Pentium III class) low-power processor and supports standard input/output devices including 10/100 MBit/s ethernet. When enclosed in the housing, the on-board computer may be accessed via ethernet through a wet-matable connector; however, experiments are performed without a tether. Executables and data are stored on an IBM 1 GB Microdrive. The processor board includes two serial ports which are used to control the daisy-chained Animatics motors and to read data from the dynamic measurement unit.

The PC/104 stack also includes an input/output board (Diamond Systems’ Model MM-32-AT) which features 32 16-bit single-ended analog input channels (reconfigurable as differential input channels), 4 12-bit analog output channels, and 24 programmable digital input/output channels.

The stack is powered by Diamond Systems’ Jupiter-MM-SIO power supply. This power supply board includes two additional serial ports, which increases the flexibility of the on-board computer.

Power. All components contained within the spherical module are powered by a Lithium-Ion battery pack assembled by EAC Corporation. The pack provides 5500 mAh of power at a nominal voltage of 28.8 VDC. Internal circuitry limits the output current to 10 A. Power is provided independently to the three reaction wheel motors, the ballast actuator motor, and the PC/104 stack.

4. CONCLUSION

This paper describes modeling and design of the Internally Actuated, Modular Bodied, Untethered Submersible (IAMBUS). This laboratory-scale vehicle provides a platform for investigating vehicle control using internal actuators. The base module is a spherical pressure housing containing three reaction wheel actuators. In this basic configuration, IAMBUS provides a unique facility for testing spacecraft attitude control schemes. Early experimental plans include a comparison of various optimal reorientation strategies (Junkins and Turner, 1986; Scrivener and Thompson, 1994). Future plans include the development of additional internal actuator modules, such as a moving mass actuator

module and a control moment gyroscope module. Plans also include the fabrication of a streamlined external fairing, with dedicated power and propulsion, which will allow experimental validation of internal actuator control strategies for AUV's.

Acknowledgements. The authors gratefully acknowledge the input and assistance of L. Elliott, N. Lambeth, M. Metheny, C. Nickell, M. Pressl, Prof. C. D. Hall, Prof. G. Kirk, and Dr. W. Hallauer. The authors also thank the anonymous reviewers for their valuable suggestions.

REFERENCES

- Eterno, J. S., R. O. Zermuehlen and H. F. Zimbelman (1995). *Space Mission Analysis and Design*. Chap. 11.1 Attitude Determination and Control, pp. 340–366. Second ed.. Microcosm, Inc. and Kluwer Academic Publishers. Boston, MA. W. J. Larson and J. R. Wertz, Eds.
- Hobson, B., M. Kemp and A. Leonessa (2002). Integration of a hovering module on to the Morpheus AUV: Application to MCM missions. In: *MTS/IEEE OCEANS 2002*. Biloxi, MS. pp. 207–209.
- Junkins, J. L. and J. Turner (1986). *Optimal Spacecraft Rotational Maneuvers*. Elsevier. New York, NY.
- Kato, N. and I. Tadahiko (1998). Guidance and control of fish robot with apparatus of pectoral fin motion. In: *Proc. International Conference on Robotics and Automation*. Leuven, Belgium. pp. 446–451.
- Lamb, H. (1932). *Hydrodynamics*. 6th ed.. Dover. New York.
- Leonard, N. E. and J. G. Graver (2001). Stabilizing underwater vehicle motion using internal rotors. *IEEE J. Oceanic Engineering* **326**(4), 633–645.
- Schwartz, J. L., M. A. Peck and C. D. Hall (2003). Historical review of spacecraft simulators. In: *Proc. 2003 AAS/AIAA Space Flight Mechanics Conference*. Ponce, Puerto Rico.
- Scrivener, S. L. and R. C. Thompson (1994). Survey of time-optimal attitude maneuvers. *Journal of Guidance, Control, and Dynamics* **17**(2), 225–233.
- Woolsey, C. A. and N. E. Leonard (2002). Stabilizing underwater vehicle motion using internal rotors. *Automatica* **38**(12), 2053–2062.